

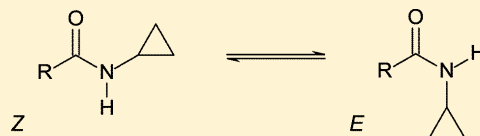
Conformational Features of Secondary *N*-Cyclopropyl Amides

Ángela González-de-Castro, Howard Broughton, José A. Martínez-Pérez,* and Juan F. Espinosa*

Centro de Investigación Lilly, Avda. de la Industria, 30, 28108-Alcobendas, Madrid, Spain

Supporting Information

ABSTRACT: NMR studies in conjunction with *ab initio* calculations revealed unexpected conformational behavior of *N*-cyclopropylacetamide (**1**). This secondary amide displays 16–19% *E*-rotamer (*cis*) around the carbonyl–nitrogen bond in apolar solvents, in contrast to other aliphatic secondary acetamides in which significant *E*-rotamer populations are rare due to steric contacts between the substituents on the amide bond. In addition, **1** adopts an *ortho* conformation around the *N*–cPr bond instead of the *anti* conformation generally preferred by secondary acetamides. This distinct conformational behavior was also observed for other secondary *N*-cyclopropyl amides.



INTRODUCTION

Secondary amides generally exist as a predominant *Z*-rotamer (or *trans*) to avoid steric clash between groups attached to the carbonyl carbon and the nitrogen.¹ For instance, when both substituents are methyl groups (*N*-methylacetamide) the population of the most stable *Z*-rotamer is 98.5%.² This strong preference is reflected in the scarcity of *E*-rotamers (or *cis*) around secondary amide bonds in protein backbones^{3–5} while the fraction of *cis* peptide bonds of prolines is significantly higher (5–9%).^{6,7} These *cis* peptide bonds are usually critical to regulate biochemical processes and are located near the active sites of proteins.^{8,9} When the peptide bond is *cis*, one of the amino acids is typically aromatic, suggesting that CH– π interactions may stabilize the *cis* conformation.¹⁰

Cis secondary amides have been observed within host–guest complexes when the energetic cost associated with the *cis* rotamer is compensated by the occurrence of intermolecular hydrogen bonds between the components of a supramolecular assembly.^{11–13} An increase in the *cis* rotamer population has been also observed in secondary amides in which this rotamer is stabilized by noncovalent interactions between the amide substituents. Gellman and co-workers developed a propargylic secondary amide that displayed 24% *cis* rotamer in aqueous solution in part due to the low steric bulk of the propargylic moiety and in part due to the hydrophobic effect arising from the clustering of the aromatic rings of the substituents on the amide bond.¹⁴ Smith and co-workers showed that *N*-(pyrimidin-2-yl) pentafluorobenzamide, in which the *cis* rotamer is apparently stabilized by an interaction between the nitrogen lone pair and the pentafluorophenyl ring, existed as the *cis* amide in the solid state and as a solvent-dependent mixture of *cis* and *trans* rotamers in solution.¹⁵

The conformation around the *N*-alkyl bond, which has been the subject of theoretical and experimental analysis, is also worthy of consideration. *Ab initio* calculations predicted the *anti* conformer, in which the NH and CH bonds form a dihedral angle of 180°, as the lowest in energy for both *Z*- and *E*-rotamers in a series of acetamides.¹⁶ The *anti* conformation around the *N*-alkyl bond was confirmed on the basis of the

chemical shift of the *N*-CH α proton, which is deshielded about 0.8 ppm by the carbonyl group. A predictive algorithm that correlated DFT-calculated structures and proton chemical shifts of the CH α proton was developed.¹⁷ The analysis of the X-ray crystal structures of simple amides and small peptides indicated that the conformations adopted by the secondary amides in the solid state are very similar in general to the *anti* conformers found in the gas phase and in solution.¹⁸

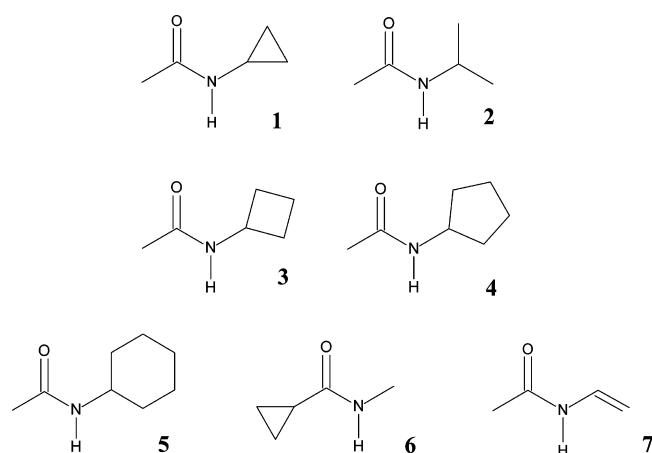
In this context, we observed that *N*-cyclopropylacetamide (**1**), a small aliphatic secondary amide for which only a very predominant *trans* rotamer was expected, displayed 19% *cis* rotamer in CDCl₃, which is a significant population in comparison to the low or undetectable *cis* rotamer population reported for other aliphatic secondary amides. Additional NMR studies revealed further conformational differences around the *N*-cPr bond as the NH and CH bonds form a dihedral angle of about 100° (*ortho* conformer) instead of the value of 180° (*anti* conformer) observed for other secondary amides. These experimental findings were in agreement with the conformational preferences predicted by *ab initio* calculations.

RESULTS AND DISCUSSION

The ¹H spectrum of *N*-cyclopropylacetamide (**1**) showed two sets of proton signals in CDCl₃ at 298 K in an ~81:19 ratio (Figure 1). The signal ratio changed to ~96:4 in DMSO-*d*₆, where the signals merged to one set after warming to 393 K (data not shown). The original two sets were recovered upon cooling and equilibration. The solvent-dependent ratio and the reversible changes with temperature were in favor of the presence of two rotamers around the amide bond in slow equilibrium on the chemical shift time scale. A 2D-EXSY experiment,¹⁹ in which exchange peaks between the resonances of the species were observed, provided further evidence of the two interconverting rotamers (Figure 2).²⁰ The *Z/E* assignment was achieved based on proton and carbon chemical shift differences between rotamers, since it is well established that in

Received: February 1, 2015

Published: March 24, 2015



an amide the carbonyl bond anisotropy produces a deshielding effect on protons and a shielding effect on carbons of the same side.²¹ The major species corresponds to the *Z*-rotamer (*trans*). The *E*-rotamer population for **1** in CDCl₃ at 298 K (18.7%) contrasts with that of the acyclic analogue bearing an isopropyl group on the nitrogen (**2**), which only displayed 2.5% *E*-rotamer population in the same solvent. Rotamer ratios were used to determine the free energy difference ($\Delta G_{Z/E}$) between rotamers at 298 K in CDCl₃ according to the Boltzmann distribution. In **2**, the *Z*-rotamer is 2.2 kcal/mol more stable than the *E*-rotamer while in **1** it is only 0.88 kcal/mol more stable.

To ascertain the influence of ring size on the rotamer ratio, the *Z/E* ratios for acetamides **3–5**, with other alicyclic rings attached to the nitrogen, were determined in CDCl₃. The *E*-rotamer population was 5.5% for *N*-cyclobutyl (**3**), 4.6% for *N*-cyclopentyl (**4**), and 3.7% for *N*-cyclohexyl (**5**) acetamides (see Supporting Information), indicating an inverse relationship between *E*-rotamer population and ring size, which suggested that the significant *E*-rotamer population of **1** could be a consequence of the small steric hindrance between the cyclopropyl and methyl groups. However, the low *E*-rotamer population (1.5%) measured for the reverse amide **6**, in which the positions of the cyclopropyl and methyl groups are interchanged, suggested that the unusual *E*-rotamer population is not dictated by just steric considerations. Since, according to the Walsh model,²² cyclopropyl carbons have substantial sp² character, the rotamer equilibrium of *N*-vinyl acetamide **7** was investigated because this secondary amide may represent a closer analogue of **1** than aliphatic acetamides. However, only a low population of the *E*-rotamer (4.7%) was detected for **7**,

suggesting that the stabilization of the *cis* rotamer cannot be attributed to an increase in the sp² character of the carbon attached to the amide bond either. The chemical shifts of the relevant proton resonances for the *Z*- and *E*- rotamers of amides **1–7** are collected in Table 1.

Next, to shed light on the origin of the significant *E*-rotamer population, we investigated the influence of several factors, such as temperature, concentration, and solvent polarity, on the rotamer equilibrium of **1**. Several spectra were acquired from 233 to 303 K in CDCl₃, and we found that the rotamer ratio was essentially insensitive to temperature, reflecting a negligible entropic contribution to *Z/E* isomerization, in contrast to the temperature-dependent ratio observed for secondary amides in which the *E*-rotamer is stabilized by the hydrophobic effect.^{14,15} Furthermore, the effect of concentration was examined and the rotamer ratio remained constant over the 40–0.4 mM concentration range, discarding the possibility of formation of intermolecular assemblies. However, the rotamer ratio of **1** showed a clear solvent dependence, and the *E*-rotamer fraction increased from 4% to 8% in polar solvents to 16–19% in apolar solvents (Figure 3), while the rotamer ratio of **2** was practically independent of solvent polarity (data not shown). This finding suggested the existence of an electrostatic interaction that stabilizes the *E*-rotamer, and/or destabilizes the *Z*-rotamer of **1** in nonpolar solvents. In polar media, this electrostatic interaction would be attenuated by the solvent and the equilibrium seems to be governed by steric factors.

The NMR analysis provided additional insights into the conformational behavior of **1** around the N–cPr bond through the analysis of the NH–CH coupling constant across this bond. Aliphatic acetamides arrange the NH proton in an *anti* disposition with respect to the CH proton,^{16,17} and a large NH–CH coupling constant would be expected according to the Karplus–Altona equation.²³ For instance, the large ³J_{NH–HC} values measured for **2** (7.4 Hz for both rotamers) and **3** (8.1 and 8.3 Hz for the *E*- and *Z*-rotamers respectively) in CDCl₃ are consistent with the predominance of the *anti* conformer around the N–cPr bond. In contrast, small ³J_{NH–HC} values were derived for **1** (1.5 and 2.7 Hz for the *E*- and *Z*- rotamers respectively) from ¹H NMR homonuclear decoupling experiments, where the multiplicity of the cyclopropyl CH signal was simplified to allow for easy measurement of the coupling constant (Figure 4). This significant difference in the NH–CH coupling constant reflects a conformational change around the N–cPr bond of **1** relative to other acetamides such as **2** and **3**. The experimental ³J_{NH–HC} values of both rotamers of **1** were similar in all the solvents tested, highlighting a strong

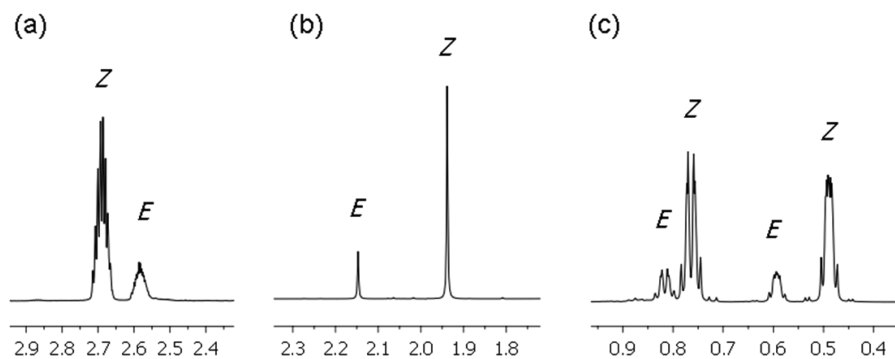


Figure 1. Expansions of the ¹H spectrum of **1** in CDCl₃ at 298 K showing the CH (a), CH₃ (b), and CH₂ (c) resonances of the *Z* and *E* rotamers of **1**. The *Z/E* ratio is 81:19.

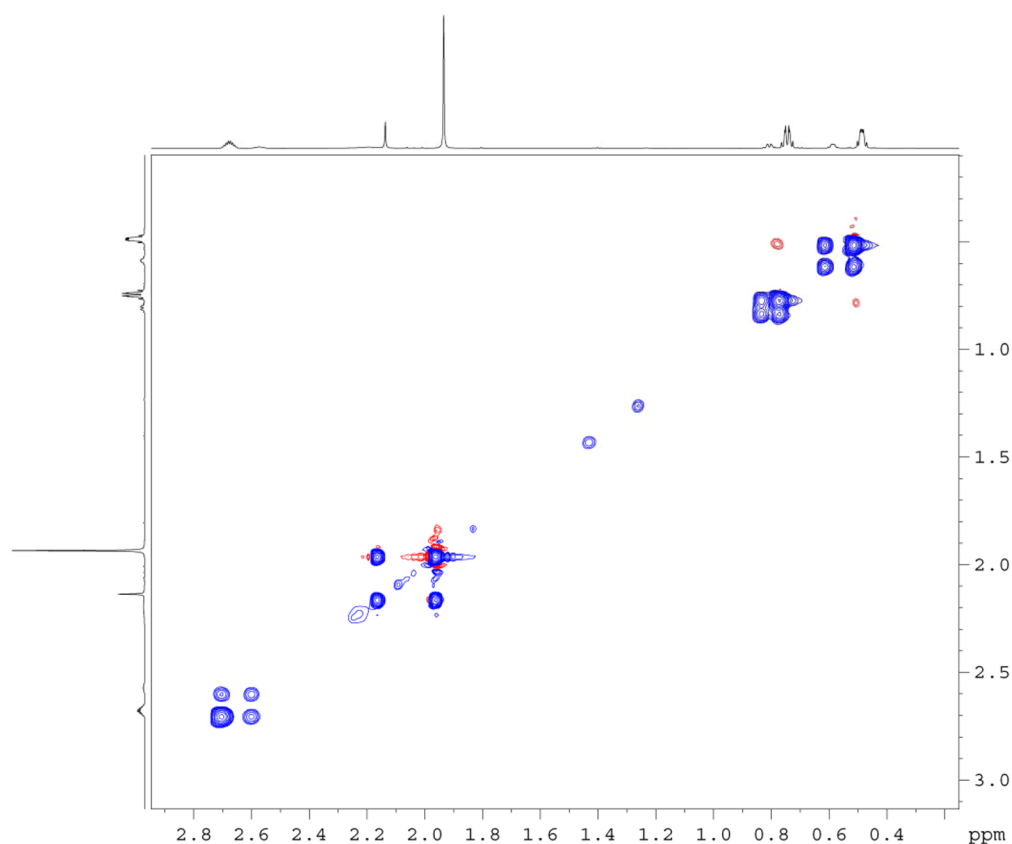


Figure 2. Expansion of the 2D-EXSY spectrum of **1** in CDCl_3 at 298 K showing exchange cross-peaks between rotamer resonances of the same sign as the diagonal.

Table 1. Chemical Shifts (in ppm) for Selected Proton Resonances of Compounds 1–7

| compd | rotamer | $\text{H}\alpha$ | HN | CH_3 |
|-------|---------|------------------|----------|---------------|
| 1 | Z | 2.68 | 5.9 | 1.94 |
| | E | 2.57 | 5.74 | 2.14 |
| 2 | Z | 4.00 | 5.86 | 1.89 |
| | E | 3.60 | 5.39 | 1.99 |
| 3 | Z | 4.37 | 5.94 | 1.93 |
| | E | 3.92 | 5.61 | 1.96 |
| 4 | Z | 4.19 | 5.52 | 1.95 |
| | E | 3.81 | <i>a</i> | 2.06 |
| 5 | Z | 3.76 | 5.67 | 2.00 |
| | E | 3.24 | <i>a</i> | 2.24 |
| 6 | Z | 1.35 | 5.97 | 2.80 |
| | E | 1.63 | <i>a</i> | 3.03 |
| 7 | Z | 6.93 | 7.94 | 2.02 |
| | E | 6.47 | 7.54 | 2.11 |

^aNot determined.

conformational preference around the N–CPr bond that is not affected by the solvent. Additional information can be extracted from $\text{H}\alpha$ chemical shifts, which have been used as a diagnostic probe for assignment of rotamers in amides because they are sensitive to the carbonyl bond anisotropy.¹⁷ Thus, the difference between the $\text{H}\alpha$ chemical shifts of the Z- and E-rotamers reflects the magnetic deshielding generated by the carbonyl bond and can be used to determine the disposition of the $\text{H}\alpha$ relative to the carbonyl moiety. While this chemical shift difference is between 0.4 and 0.5 ppm for **2–5**, which is consistent with the Z-anti conformer where the $\text{H}\alpha$ lies in the

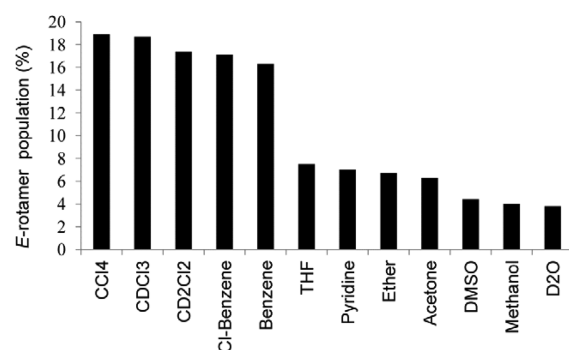


Figure 3. Relative population for the E-rotamer of **1** in several deuterated solvents at 298 K.

plane defined by the HN–CO moiety and on the same side as the carbonyl group, the difference is only *ca.* 0.1 ppm for **1**, reflecting the fact that the $\text{H}\alpha$ is out of the plane of the HN–CO moiety, in agreement with the conformational change inferred from proton–proton coupling constants.

To further understand the conformational differences between **1** and other aliphatic acetamides, *ab initio*/DFT calculations were carried out for the Z- and E-rotamers of **1–3**. Low-energy conformers were identified through a conformational search with molecular mechanics calculations and subjected to geometry optimization with Gaussian 03 software²⁴ in the gas phase at the B3LYP/6-311++G** level of theory. The relative energies were then used to compute Boltzmann populations. Remarkably, the calculations predicted that the E-rotamer population of **1** is 19.0%, whereas this rotamer is expected to be barely populated in **2** (0.9%) and **3**

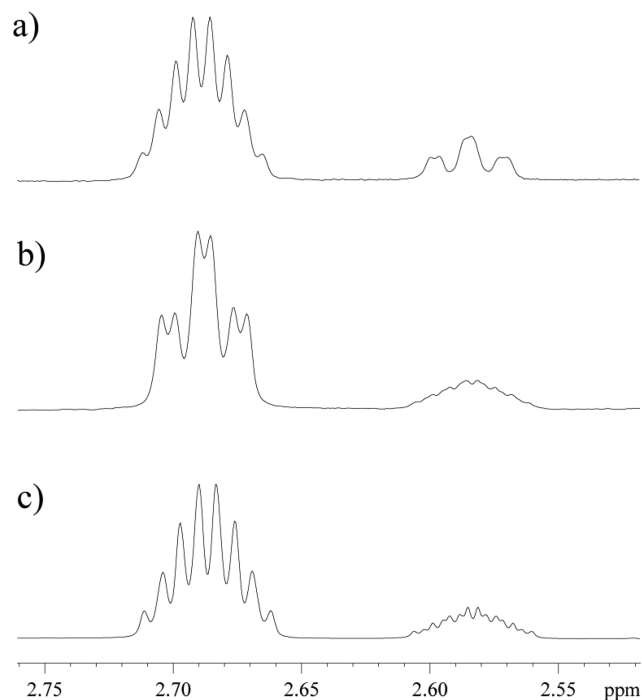
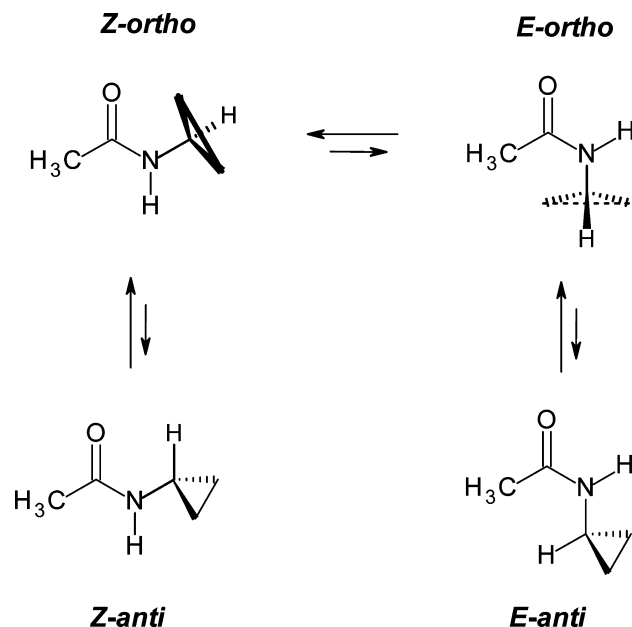


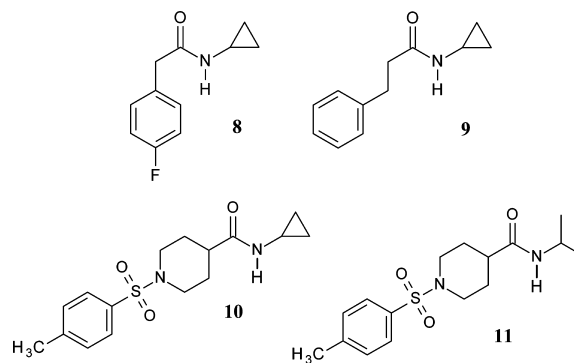
Figure 4. Multiplicity of the CH cyclopropyl resonance of both rotamers of **1** in homonuclear decoupling spectra (a,b) relative to the ¹H spectrum (c). The CH₂ cyclopropyl resonance at lower chemical shift of the *E*-rotamer (a) or of the *Z*-rotamer (b) was irradiated. The spectra were acquired in CDCl₃.

(1.8%), in agreement with the experimental findings in apolar solvents. Furthermore, the *ab initio* calculations revealed a conformational change around the N–cPr bond of **1** with respect to the N-alkyl or N-cycloalkyl bonds of **2** and **3**, as previously deduced from the NH–CH coupling constants. The *anti* conformer, in which the N–H and C–H bonds form a dihedral angle of ~180°, is the most abundant conformer for both rotamers of **2** and **3** as described for other N-alkyl acetamides.^{16,17} In contrast, the *ortho* conformer, in which the N–H and C–H bonds form a dihedral angle of ~100°, is the preferred conformation for both rotamers of **1** (Scheme 1). The theoretical NH–CH coupling constants were determined by *ab initio* methods for the lowest-energy conformer of **1–3**. A small ³J_{NH-CH} was calculated for **1** (0.5 Hz), and large coupling constants were determined for **2** (7.8 Hz) and **3** (9.7 Hz). The calculated couplings are similar to the experimental values, in agreement with the predominance of the *ortho* conformer around the N–cPr bond of **1**, whereas the *anti* conformer is preferred for **2** and **3**. In addition, *ab initio*/DFT calculations were carried out in chloroform and DMSO PCM solvent models²⁵ in an attempt to examine the influence of solvent polarity on the rotamer equilibrium. A comparison between the populations derived from the *ab initio* energies and those determined by NMR is shown in Figure 5. For **2** and **3** the *ab initio* calculations yielded very similar results in CDCl₃ and DMSO, and only a very low population of the *E*-rotamer is predicted, which is consistent with the experimental results. In contrast, a significant population of the *E*-rotamer is predicted for **1** in both solvents, and this population is higher in CDCl₃ than in DMSO, which follows the experimental trend, although the experimental values are lower than those predicted by the calculations.

Scheme 1. Scheme of the Conformational Equilibrium of **1** Depicting the *E*- and *Z*-Rotamers around the N–CO Bond and the *anti* and *ortho* Conformers around the N–cPr Bond



To determine whether the unusual *Z*/*E* rotamer ratio was specific for **1** or also occurred for other secondary N-cyclopropyl amides, we investigated the rotamer ratio for amides **8–11** in CDCl₃. We found that **8** and **9**, with R–CH₂ moieties attached to the carbonyl carbon, showed considerable *E*-rotamer populations (15% and 8% respectively), indicating that the conformational effect exerted by the cyclopropyl ring is not limited to acetamides. A similar conclusion was achieved through the comparison of the rotamer equilibrium of **10** and **11**, since N-cPr amide **10**, with a bulky substituent on the carbonyl carbon, showed 5% *E*-rotamer population, whereas this rotamer was not detected for the corresponding N-iPr amide **11**, resembling the behavior of the **1–2** pair. In addition, analysis of the multiplicity of the CH cyclopropyl resonance of **8–10** revealed a small NH–CH coupling constant for the three N-cyclopropyl amides, reflecting an *ortho* conformation around the N–cPr bond as described for **1**.



Finally, a search in the Crystallographic Cambridge Database²⁶ aimed at examining the conformational preferences of secondary N-cyclopropyl amides in crystals yielded five structures. All of them correspond to the major *Z*-rotamer and exhibit the *ortho* conformation around the N–cPr bond (HN–CH torsion angles between 113° and 133°), indicating a

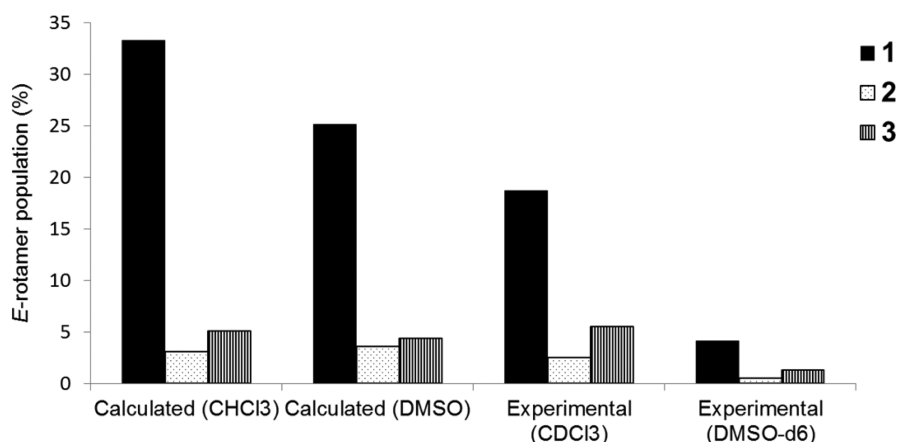


Figure 5. Experimental and *ab initio* calculated *E*-rotamer populations in chloroform and DMSO for acetamides 1–3.

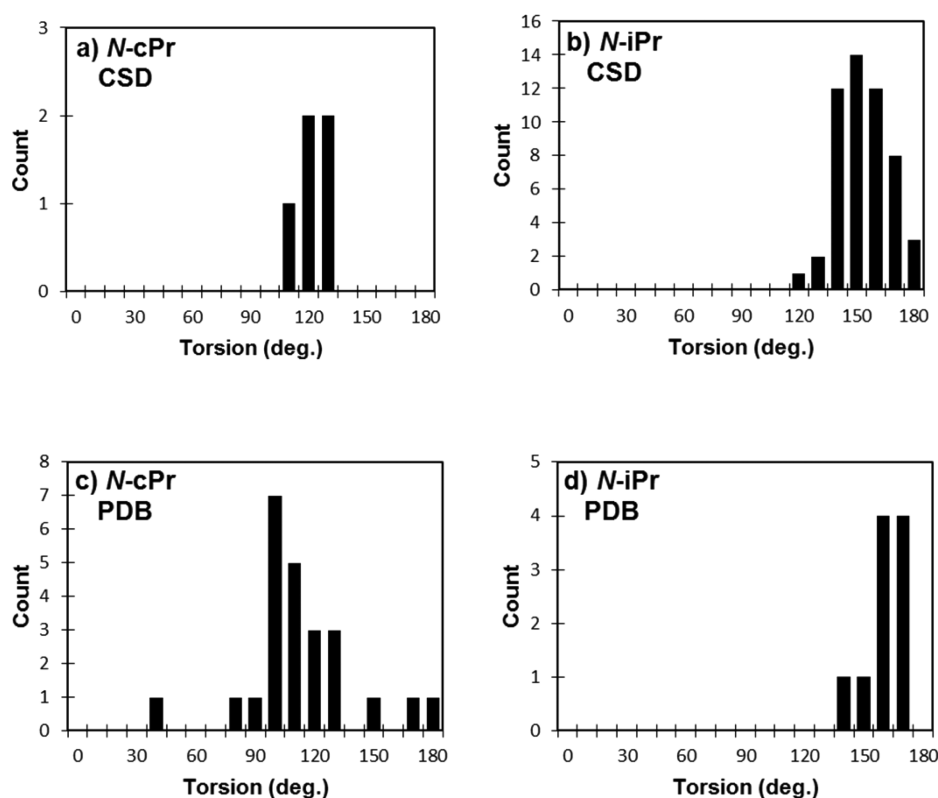


Figure 6. Conformational histograms of secondary *N*-cyclopropyl (a,c) and *N*-isopropyl (b,d) amides derived from CSD (a,b) and PDB (c,d) X-ray structures as a function of the HN–CH dihedral angle. The torsion values were binned in 10° intervals, and the number of occurrences of each torsion range (indicated value $\pm 5^\circ$) is given on the left axis. For simplicity, the mirror-image conformations at torsion angles $\pm \tau$ were binned together to reduce the range of the torsion angles in the histogram from 0° to 180°.

good correspondence between the conformational preferences in solution and in the solid state. This is in stark contrast with the predominance of *Z-anti* conformations (HN–CH torsion angles between 135° and 180°) for secondary *N*-isopropyl amides (49 out of 52 cases). Furthermore, secondary amides are often involved in protein–ligand interactions and a search in the Protein Data Bank²⁷ identified the structures of 24 secondary *N*-cyclopropyl amides bound to proteins. The majority of them also adopt the *Z-ortho* conformer in the protein binding site (20 out of 24 cases), while the *Z-anti* form was the crystallographic conformation for all 10 secondary *N*-isopropyl amides in this database. The conformational preferences around the HN–CH bond observed in the crystal

structures of free and bound secondary *N*-cPr and *N*-iPr amides are represented using conformational histograms²⁸ in which the torsion values are binned in intervals and the abundance (count) of each torsional range is shown (Figure 6).

CONCLUSIONS

NMR data reveal that the rotamer equilibrium of *N*-cyclopropyl acetamide 1 and other secondary *N*-cyclopropyl amides in apolar solvents shows a significant *E*-rotamer population, differing from other aliphatic secondary amides for which the *Z*-rotamer is practically the only populated rotamer in solution. Remarkably, the conformational differences are not only restricted to the amide bond because *N*-cyclopropyl amides

adopt an *ortho* conformation around the N–cPr bond in contrast to the *anti* arrangement reported for other acetamides. *Ab initio* calculations at the B3LYP/6-311++G** level were shown to be capable of predicting the lower energy difference between rotamers in **1** relative to other acetamides, as well as the predominance of the *ortho* conformer. Based upon experimental data (particularly solvent effects) and the outcome of theoretical predictions, we believe that the most important factors controlling the conformational behavior of secondary N-cyclopropyl acetamides are electrostatics and hyperconjugation, with steric factors playing a less important role.

Over 500 N-cyclopropyl amides have been described for their effect on biological systems, and this motif is currently present in a launched drug and in five clinical molecules according to the MDDR database.²⁹ Advantages of the N-cyclopropyl group in amides for reducing metabolism³⁰ or increasing hydrogen bond capacity³¹ have been reported. In this work we demonstrate that the presence of the N-cyclopropyl group has conformational implications as well.³²

EXPERIMENTAL SECTION

All the secondary amides described in this study are commercially available. NMR samples of the compounds were prepared at 0.4, 4, and 40 mM (**1**) and at 4 mM (**2–11**) in CDCl₃. Additional samples of **1** and **2** were prepared at 4 mM in several solvents (CCl₄, CD₂Cl₂, chlorobenzene-d₅, benzene-d₆, THF-d₈, pyridine-d₅, diethyl ether-d₁₀, acetone-d₆, DMSO-d₆, methanol-d₄, and D₂O). All the NMR spectra were acquired on a 500 MHz spectrometer equipped with a 5 mm inverse probe. Proton and carbon chemical shifts were referenced to the residual solvent signals. ¹H and ¹³C spectra were acquired using 32K data points and zero-filled to 64K. Spectra were acquired at 25 °C for **2–11** and between –40 and 40 °C in CDCl₃ for **1**. A phase-sensitive Heteronuclear Single Quantum Coherence (¹H–¹³C HSQC) spectrum was acquired for **1** using gradient selection techniques and an acquisition data matrix defined by 1K × 256 points in F2 and F1 respectively. Proton Homonuclear Decoupling experiments were performed by irradiating the low-frequency signal of the CH₂ protons of the cyclopropyl ring. 1D-EXSY experiments were carried out for **1–11** with the double-pulse field gradient spin echo module³³ and 2D-EXSY experiments with the conventional NOESY pulse sequence using a mixing time of 1 s.

The identification of the protons signals of the minor *cis* rotamer was achieved by simple inspection of the ¹H spectrum, and the rotamer ratio was determined by signal integration. The observation of exchange cross-peaks between the minor and major sets of signals in EXSY experiments provided confirmation of the rotameric equilibrium. For amides lacking the cyclopropyl ring in which the equilibrium was almost quantitatively shifted toward the *trans* rotamer, the position of the peaks corresponding to the *cis* rotamer was sometimes unclear, and the signals of the minor *cis* rotamer were identified through the exchange observed in 1D-EXSY experiments when the signals of the major *trans* rotamer were selectively excited.²⁰ In these latter cases, the relative integration of resonances was not accurate owing to the strong differences between signal intensities. The precision with which the rotamer ratio was quantified was improved by integration of a signal of the minor rotamer and comparison to the integral of the ¹³C-satellite peak of the corresponding signal of the major rotamer.³⁴

Density functional calculations for the prediction of conformational energies were carried out by using the Gaussian 03 software package²⁴ for **1**, **2**, and **3**. Initial conformations were generated using the MacroModel conformational search method as implemented in Maestro³⁵ with the OPLS_2005 force field.³⁶ The low-energy conformations were then subjected to DFT geometry optimization using B3LYP/6-311++G** as the basis set with tight SCF convergence criteria. The *ab initio* calculations were performed in

vacuum and in two different PCM models of solvation (CHCl₃ and DMSO).²⁵ The relative SCF energies calculated for these compounds were then used to compute the expected Boltzmann populations. The optimized structures were submitted to the NMR calculation by using the same DFT method, basis set, convergence criteria, and solvation model, and the spin–spin coupling constants were computed with the SpinSpin keyword in Gaussian 03.³⁷

The ConQuest program³⁸ (version 1.16) was used to identify the X-ray structures of secondary N-cPr and N-iPr amides in the Cambridge Crystallographic Database. Structures containing ions, metallic atoms, errors, or polymers were discarded, as were disordered structures or those solved from powder X-ray diffractograms. All the structures with determined 3D coordinates were considered for N-cPr amides, and only those with an R-factor below 0.05 were retained for N-iPr amides. Several copies of a structure in a given CSD entry were considered as independent conformations. The Relibase+ program³⁹ (version 3.2.1) was used to search the structures of secondary N-cPr and N-iPr amides complexed with proteins in the Protein Data Bank.

ASSOCIATED CONTENT

Supporting Information

¹H, ¹³C, ¹H–¹³C HSQC spectra of N-cyclopropylacetamide (**1**) in CDCl₃, ¹H spectra of secondary amides **3**, **4**, **5**, **8**, and **9** in CDCl₃, tables of atom coordinates and absolute energies of the minima obtained in the *ab initio* calculations and reference codes for the crystal structures of the Cambridge Structural Database and Protein Data Bank used to build the conformational histograms. This material is available free of charge via the Internet at <http://pubs.acs.org>.

AUTHOR INFORMATION

Corresponding Authors

*E-mail: jfespinoza@lilly.com.

*E-mail: j.martinez@lilly.com.

Notes

The authors declare no competing financial interest.

ACKNOWLEDGMENTS

The authors thank Jesus Ezquerra and Jose Alfredo Martín for useful comments and Carlos Perez Martinez for the analysis of the crystallographic databases.

REFERENCES

- (1) Stewart, W. E.; Siddall, T. H. *Chem. Rev.* **1970**, *70*, 517–551.
- (2) Radzicka, A.; Pedersen, L.; Wolfenden, R. *Biochemistry* **1988**, *27*, 4538–4541.
- (3) Mathieu, S.; Poteau, R.; Trinquier, G. *J. Phys. Chem. B* **2008**, *112*, 7894–7902.
- (4) Nguyen, K.; Iskandar, M.; Rabenstein, D. L. *J. Phys. Chem. B* **2010**, *114*, 3387–3392.
- (5) Zhang, J.; Germann, M. W. *Biopolymers* **2011**, *95*, 755–762.
- (6) Scherer, G.; Kramer, M. L.; Schutkowski, M.; Reimer, U.; Fischer, G. *J. Am. Chem. Soc.* **1998**, *120*, 5568–5574.
- (7) Weiss, M. S.; Jabs, A.; Hilgenfeld, R. *Nat. Struct. Biol.* **1998**, *5*, 676.
- (8) Chevrier, B.; Schalk, C.; D'Orchymont, H.; Rondeau, J.-M.; Moras, D.; Tarnus, C. *Structure* **1994**, *2*, 283–291.
- (9) Auffhammer, S. W.; Warkentin, E.; Ermler, U.; Hagemeyer, C. H.; Thauer, R. K.; Shima, S. *Protein Sci.* **2005**, *14*, 1840–1849.
- (10) Jabs, A.; Weiss, M. S.; Hilgenfeld, R. *J. Mol. Biol.* **1999**, *286*, 291–304.
- (11) Deetz, M. J.; Fahey, J. E.; Smith, B. D. *J. Phys. Org. Chem.* **2001**, *14*, 463–467.
- (12) Beijer, F. H.; Sijbesma, R. P.; Vekemans, J. A. J. M.; Meijer, E. W.; Kooijman, H.; Spek, A. L. *J. Org. Chem.* **1996**, *61*, 6371–6380.

- (13) Pernía, G. J.; Kilburn, J. D.; Essex, J. W.; Mortishire-Smith, R. J.; Rowley, M. *J. Am. Chem. Soc.* **1996**, *118*, 10220–10227.
- (14) Gardner, R. R.; McKay, S. L.; Gellman, S. H. *Org. Lett.* **2000**, *2*, 2335–2338.
- (15) Forbes, C. C.; Beatty, A. M.; Smith, B. D. *Org. Lett.* **2001**, *3*, 3595–3598.
- (16) Avalos, M.; Babiano, R.; Barneto, J. L.; Bravo, J. L.; Cintas, P.; Jiménez, J. L.; Palacios, J. C. *J. Org. Chem.* **2001**, *66*, 7275–7282.
- (17) Avalos, M.; Babiano, R.; Barneto, J. L.; Cintas, P.; Clemente, F. R.; Jiménez, J. L.; Palacios, J. C. *J. Org. Chem.* **2003**, *68*, 1834–1842.
- (18) Hagler, A. T.; Leiserowitz, L.; Tuval, M. *J. Am. Chem. Soc.* **1976**, *98*, 4600–4612.
- (19) Jeener, J.; Meier, B. H.; Bachmann, P.; Ernst, R. R. *J. Chem. Phys.* **1979**, *71*, 4546–4553.
- (20) Hu, D. X.; Grice, P.; Ley, S. V. *J. Org. Chem.* **2012**, *77*, 5198–5202.
- (21) Pretsch, E.; Bühlmann, P.; Affolter, C. *Structure determination of organic compounds. Tables of spectra data*; Springer: Berlin, 2000.
- (22) Walsh, A. D. *Trans. Faraday Soc.* **1949**, *45*, 179–190.
- (23) Haasnoot, C. A. G.; de Leeuw, F. A. A. M.; Altona, C. *Tetrahedron* **1980**, *36*, 2783–2792.
- (24) Frisch, M. J.; Trucks, G. W.; Schlegel, H. B.; Scuseria, G. E.; Robb, M. A.; Cheeseman, J. R.; Montgomery, J. A. Jr.; Vreven, T.; Kudin, K. N.; Burant, J. C.; Millam, J. M.; Iyengar, S. S.; Tomasi, J.; Barone, V.; Mennucci, B.; Cossi, M.; Scalmani, G.; Rega, N.; Petersson, G. A.; Nakatsuji, H.; Hada, M.; Ehara, M.; Toyota, K.; Fukuda, R.; Hasegawa, J.; Ishida, M.; Nakajima, T.; Honda, Y.; Kitao, O.; Nakai, H.; Klene, M.; Li, X.; Knox, J. E.; Hratchian, H. P.; Cross, J. B.; Bakken, V.; Adamo, C.; Jaramillo, J.; Gomperts, R.; Stratmann, R. E.; Yazyev, O.; Austin, A. J.; Cammi, R.; Pomelli, C.; Ochterski, J. W.; Ayala, P. Y.; Morokuma, K.; Voth, G. A.; Salvador, P.; Dannenberg, J. J.; Zakrzewski, V. G.; Dapprich, S.; Daniels, A. D.; Strain, M. C.; Farkas, O.; Malick, D. K.; Rabuck, A. D.; Raghavachari, K.; Foresman, J. B.; Ortiz, J. V.; Cui, Q.; Baboul, A. G.; Clifford, S.; Cioslowski, J.; Stefanov, B. B.; Liu, G.; Liashenko, A.; Piskorz, P.; Komaromi, I.; Martin, R. L.; Fox, D. J.; Keith, T.; Al-Laham, M. A.; Peng, C. Y.; Nanayakkara, A.; Challacombe, M.; Gill, P. M. W.; Johnson, B.; Chen, W.; Wong, M. W.; Gonzalez, C.; Pople, J. A. *Gaussian 03*, revision D.01; Gaussian Inc.: Wallingford, CT, 2004.
- (25) For a review of solvation methods, see: (a) Tomasi, J.; Mennucci, B.; Cammi, R. *Chem. Rev.* **2005**, *105*, 2999–3093. (b) Tomasi, J.; Mennucci, B.; Cancès, E. *J. Mol. Struct. (THEOCHEM)* **1999**, *464*, 211–226.
- (26) *Cambridge Crystallographic Database*, version 5.35 (November 2013).
- (27) The *Protein Data Bank* (www.rcsb.org), Berman, H. M., Westbrook, J.; Feng, Z.; Gilliland, G.; Bhat, T. N.; Weissig, H.; Shindyalov, I. N.; Bourne, P. E. **2000**, *Nucleic Acids Res.*, *28*, 235–242.
- (28) Hao, M.-H.; Haq, O.; Muegge, I. *J. Chem. Inf. Model* **2007**, *47*, 2242–2252.
- (29) *MDDR (Drug Data Report)*, version 2014.2. Data set is available from Accelrycs, Inc.
- (30) Arasappan, A.; Bennett, F.; Bogen, S. L.; Venkatraman, S.; Blackman, M.; Chen, K. X.; Hendrata, S.; Huang, Y.; Huelgas, R. M.; Nair, L.; Padilla, A. I.; Pan, W.; Pike, R.; Pinto, P.; Ruan, S.; Sannigrahi, M.; Velazquez, F.; Vibulbhan, B.; Wu, W.; Yang, W.; Saksena, A. K.; Girijavallabhan, V.; Shih, N.-Y.; Kong, J.; Meng, T.; Jin, Y.; Wong, J.; McNamara, P.; Prongay, A.; Madison, V.; Piwinski, J. J.; Cheng, K.-C.; Morrison, R.; Malcolm, B.; Tong, X.; Ralston, R.; Njoroge, F. G. *ACS Med. Chem. Lett.* **2010**, *1*, 64–69.
- (31) Liu, C.; Lin, J.; Wrobeski, S. T.; Lin, S.; Hynes, J., Jr.; Wu, H.; Dyckman, A. J.; Li, T.; Wityak, J.; Gillooly, K. M.; Pitt, S.; Shen, D. R.; Zhang, R. F.; McIntyre, K. W.; Salter-Cid, L.; Shuster, D. J.; Zhang, H.; Marathe, P. H.; Doweyko, A. M.; Sack, J. S.; Kiefer, S. E.; Kish, K. F.; Newitt, J. A.; McKinnon, M.; Dodd, J. H.; Barrish, J. C.; Schieven, G. L.; Leftheris, K. *J. Med. Chem.* **2010**, *53*, 6629–6639.
- (32) Preliminary data suggest a similar conformational trend for tertiary *N*-cyclopropyl amides for which the *N*-cyclopropyl group significantly increases the *E*-rotamer population relative to the analogue with an *N*-isopropyl group. For instance, 2-chloro-*N*-isopropyl-*N*-methyl-acetamide exhibits a 1:1 mixture of *Z/E* rotamers, while 2-chloro-*N*-cyclopropyl-*N*-methyl acetamide exists predominantly as the *E*-rotamer (*Z/E* ratio is 5:95).
- (33) Stott, K.; Stonehouse, J.; Keeler, J.; Hwang, T.-L.; Shaka, A. J. *J. Am. Chem. Soc.* **1995**, *117*, 4199–4200.
- (34) Claridge, T. D. W.; Davies, S. G.; Polywka, M. E. C.; Roberts, P. M.; Russell, A. J.; Savory, E. D.; Smith, A. D. *Org. Lett.* **2008**, *10*, 5433–5436.
- (35) *Maestro*, version 9.3; Schrodinger LLC: New York, NY, 2012.
- (36) *OPLS_2005*, MacroModel, version 9.9; Schrodinger, LLC: New York, NY, 2012.
- (37) (a) Helgaker, T.; Watson, M.; Handy, N. C. *J. Chem. Phys.* **2000**, *113*, 9402–9409. (b) Sychrovsky, V.; Gräfenstein, J.; Cremer, D. *J. Chem. Phys.* **2000**, *113*, 3530–3547.
- (38) Bruno, I. J.; Cole, J. C.; Edgington, P. R.; Kessler, M.; Macrae, C. F.; McCabe, P.; Pearson, J.; Taylor, R. *Acta Crystallogr.* **2002**, *B58*, 389–397.
- (39) *Relibase+*, version 3.2.1; The Cambridge Crystallographic Data Center, U.K., 1999–2011.